



Thermal properties of fully delithiated olivines

Jae-Sang Park ^{a,1}, Seung-Min Oh ^{b,1}, Yang-Kook Sun ^{b,c,*}, Seung-Taek Myung ^{a,**}

^a Department of Nano Engineering, Sejong University, Seoul 143-747, South Korea

^b Department of Energy Engineering, Hanyang University, Seoul 137-791, South Korea

^c Chemistry Department, Faculty of Science, King Abdulaziz University, Jeddah, Saudi Arabia



HIGHLIGHTS

- Carbon-coated $\text{LiMn}_x\text{Fe}_{1-x}\text{PO}_4$ ($x = 0, 0.5$ and 1) was fully delithiated using an oxidant NO_2BF_4 .
- Thermal properties of the $\text{Li}_0\text{Mn}_x\text{Fe}_{1-x}\text{PO}_4$ were studied by TG, *in situ* XRD, and DSC.
- Phase stability of the olivines was strongly affected by Mn content in the $\text{LiMn}_x\text{Fe}_{1-x}\text{PO}_4$.
- The Li_0FePO_4 was the most stable up to 500°C maintaining the original olivine structure.

ARTICLE INFO

Article history:

Received 10 December 2013

Received in revised form

9 January 2014

Accepted 9 January 2014

Available online 20 January 2014

Keywords:

Delithiation

Olivine

Thermal stability

Cathode

Lithium battery

ABSTRACT

Carbon-coated $\text{LiMn}_x\text{Fe}_{1-x}\text{PO}_4$ ($x = 0, 0.5$ and 1) is fully delithiated using NO_2BF_4 oxidant to investigate thermal behavior as a function of temperature as high as 700°C in an Ar atmosphere. Reitveld refinement of X-ray diffraction (XRD) studies indicates readiness of chemical delithiation, except for Li_0MnPO_4 , hydrated to amorphous $\text{MnPO}_4 \cdot 2\text{H}_2\text{O}$. Thermal studies coupled with thermogravimetric analysis and *in situ* high temperature XRD demonstrate that the phase stability is affected by substituted Mn at an elevated temperature. The Li_0FePO_4 is stable up to 500°C , maintaining the original olivine structure with a small amount of oxygen release. At higher temperatures, the phase was transformed to $\text{Fe}_3(\text{PO}_4)_2$ and $\text{Fe}_2\text{P}_2\text{O}_7$. In contrast, the phase transformation temperature is apparently reduced to as low as 200°C by the addition of Mn into the crystal structure, which is related to the phase transformation to $(\text{Mn}_{0.5}\text{Fe}_{0.5})_3(\text{PO}_4)_2$ associated with fast oxygen loss from the original structure. As a result, the better thermal stability of Li_0FePO_4 is attributed to less oxygen loss, which delays the phase transformation, resulting in less exothermic heat in the temperature range.

© 2014 Elsevier B.V. All rights reserved.

1. Introduction

Olivine-type LiMPO_4 compounds ($M = \text{Fe}$ and Mn) have been extensively investigated as positive electrode materials for rechargeable lithium batteries [1–5]. The stable nature in the crystal structure is supported by the $(\text{PO}_4)^3-$ -polyanion [1], which results in low electric conductivity ($10^{-8} \text{ S cm}^{-1}$) [2,4]. The Li ions are de-/intercalated at a partially elevated potential of 3.5 V versus Li/Li^+ based on the $\text{Fe}^{2+/3+}$ redox due to the presence of the P–O covalent bond in the crystal structure of the olivine compound. Accommodation of conducting carbons on olivine LiFePO_4 or cation

deficiency in the LiFePO_4 structure has led to significant progress in high-rate electrode performances [3,4] and has demonstrated use in large-format batteries such as power sources for electric vehicles and energy storage systems.

The low operation voltage of LiFePO_4 can be increased through substitution of Fe with Mn, resulting in a redox of 4.1 V versus Li/Li^+ based on $\text{Mn}^{2+/3+}$. The replacement is quite easy due to the similarity of ionic radii of Fe^{2+} and Mn^{2+} , such that a solid-solution is formed over the entire range, $\text{LiMn}_x\text{Fe}_{1-x}\text{PO}_4$ ($x = 0–1$), maintaining the olivine structure. Although LiMnPO_4 also suffers from poor electronic conductivity ($<10^{-10} \text{ S cm}^{-1}$) and short cycle life due to Mn dissolution, like the Mn spinel [6–11], Aurbach's group showed the effectiveness in carbon-coating of LiMnPO_4 with impressive cycling stability [9]. Recently, the same group suggested the best composition, carbon-coated nanoparticles of $\text{LiMn}_{0.8}\text{Fe}_{0.2}\text{PO}_4$, which exhibited the highest capacity and kinetics ever achieved [10].

More importantly, the above-mentioned olivine compounds exhibit superior thermal properties, even in a highly delithiated

* Corresponding author. Department of Energy Engineering, Hanyang University, Seoul 137-791, South Korea. Tel.: +82 2 2220 0524; fax: +82 2 2282 7329.

** Corresponding author. Tel.: +82 2 3408 3454; fax: +82 2 3408 4342.

E-mail addresses: yksun@hanyang.ac.kr, yksun7804@gmail.com (Y.-K. Sun), smyung@sejong.ac.kr (S.-T. Myung).

¹ These authors contributed equally to this work.

state. For delithiated transition metal oxides, the O₂ released from the crystal lattice can ignite the flammable electrolyte and may cause an explosion. In contrast, the strong covalent P–O bond is believed to prevent oxygen loss from olivine structures. Rousse et al. [12] observed that delithiated triphylite FePO₄ was stable up to 600 °C in air, above which it transformed into quartz-like FePO₄ without losing oxygen. The present P–O bond is stable enough to maintain the structure at such high temperatures. Chen et al. [13] revealed that delithiated Li_δMnPO₄ ($\delta < 0.16$) decomposed to form Mn₂P₂O₇ and released O₂ when heated under flowing N₂. A similar reaction for Li_{0.15}MnPO₄ occurred at a slightly lower temperature of 210 °C in an ambient vacuum state, as reported by Kim et al. [14].

Our earlier study confirmed that electrochemically delithiated carbon-coated LiFe_xMn_{1-x}PO₄ possesses stable thermal and safety properties compared to those of highly delithiated transition metal oxides [15]. The exothermic reaction range, however, was broad with increasing Mn content in Li₀Mn_xFe_{1-x}PO₄ (x to 0.85), as confirmed by a differential scanning calorimeter (DSC). The onset exothermic temperature of Mn-rich olivine is lower than that of delithiated transition metal oxides when both electrodes deliver the same capacity.

Electrochemical delithiation is available to observe the structural change, whereas full delithiation does not readily occur for Mn-doped LiFePO₄ due to poor electric conductivity (<10⁻¹⁰ S cm⁻¹), even though conducting carbon layers on the surfaces play a role in increasing the electric conductivity. The electrochemical method, thus, is not suitable for yielding fully delithiated Li₀Mn_xFe_{1-x}PO₄ ($x = 0, 0.5$ and 1). Alternatively, chemical delithiation using the NO₂BF₄ oxidant is highly effective for oxidizing these olivine compounds and is accompanied by extraction of lithium ions from the structure for charge compensation. In the present study, the chemically delithiated carbon-coated Li₀Mn_xFe_{1-x}PO₄ ($x = 0, 0.5$ and 1) is investigated to better understand its thermal behavior up to 700 °C in an Ar atmosphere.

2. Experimental

Carbon-coated LiMn_xFe_{1-x}PO₄ ($x = 0, 0.5$ and 1) was synthesized via coprecipitation. Details of the synthetic process are reported in our previous articles [16–18]. Chemical extraction of lithium from the synthesized materials was performed by NO₂BF₄ (2-fold excess versus active material) in acetonitrile for several days under an Ar atmosphere in a glove box to produce Li₀Mn_xFe_{1-x}PO₄ ($x = 0, 0.5$ and 1). The reacted products were washed several times with acetonitrile to remove LiBF₄ and were dried under Ar. The chemical compositions of the resulting powders were determined by atomic absorption spectroscopy (Analyst 300, Perkin–Elmer).

The prepared materials were subjected to analyses by X-ray diffraction (XRD), thermogravimetric analysis (TGA), and differential scanning calorimetry (DSC). The crystalline phases of the chemically delithiated products were characterized by powder XRD (Rint-2000, Rigaku) using Cu-K α radiation. The FULLPROF Rietveld program was used to analyze the powder diffraction patterns [19]. The chemically delithiated powders were subjected to TGA (loaded sample amount: 10 mg, DTG-60, SHIMADZU, Japan) combined with in situ HT-XRD (Rint-2200 and PTC-30, Rigaku, Japan). The HT-XRD patterns were collected on a Pt heating strip in Ar. For TGA, samples were thermally cycled from room temperature to 600 °C at a heating and cooling rate of 1 °C min⁻¹ and were held at select temperatures for 10 min prior to data collection. The XRD data was obtained at $2\theta = 10$ –80° with a step size of 0.03° and a count time of 0.5 s during each temperature increment. The lattice parameters were calculated by the following method: the positions of the individual peaks were fitted with a pseudo-Voigt or Lorentz function,

and typically, peak positions were input to minimize the least-squares difference between the calculated and measured peak positions by adjusting the lattice constant and vertical displacement of the sample.

In a DSC experiment, the chemically delithiated Li₀Mn_xFe_{1-x}PO₄ ($x = 0, 0.5$ and 1) powders (3–5 mg) were loaded in a stainless steel, sealed pan with a gold-plated copper seal (which could withstand 150 atm of pressure before rupturing and had a capacity of 30 μ L). These measurements were performed in a Pyris 1 calorimeter (Perkin–Elmer) at a temperature scan rate of 1 °C min⁻¹. The weight was constant in all cases, indicating that no leaks occurred during the experiments.

3. Results and discussion

To investigate the fully delithiated carbon-coated olivine Li₀Mn_xFe_{1-x}PO₄ ($x = 0, 0.5$ and 1), the most important concern is to synthesize single phase materials because undesired impurities may cause misinterpretation of the phase after the delithiation. Rietveld refinement results of XRD data for the as-synthesized carbon-coated LiMn_xFe_{1-x}PO₄ ($x = 0, 0.5$ and 1) are shown in Fig. 1. The refinement is performed assuming an orthorhombic structure with a space group of *Pnma*. The observed and calculated patterns coincide well, without impurities for the three samples. The lattice parameters of LiMn_xFe_{1-x}PO₄ ($x = 0, 0.5$, and 1) materials are calculated by the Rietveld refinement: LiFePO₄ ($a = 10.3284(2)$, $b = 6.0038(1)$, and $c = 4.6906(1)$) [16], LiMn_{0.5}Fe_{0.5}PO₄ ($a = 10.416(4)$, $b = 6.070(2)$, and $c = 4.728(2)$) [17], and LiMnPO₄ ($a = 10.4628$, $b = 6.1054$, and $c = 4.7453$) [18]. Due to the difference in the ionic radius of Fe²⁺ (0.78 Å [20]) and Mn²⁺ (0.83 Å [20]), the calculated lattice parameters increase as Mn replaces the Fe in LiFe_{1-x}Mn_xPO₄ ($x = 0.5$ and 1).

The carbon-coated LiFePO₄ was fully delithiated in one week, while the carbon-coated LiMnPO₄ reached a fully delithiated state two weeks later, as confirmed by the elemental analysis results, indicating that the extraction kinetics seem to be related to the electric conductivity of materials. Similar to the lithiated olivines, the refinements for the chemically delithiated Li₀Mn_xFe_{1-x}PO₄ ($x = 0, 0.5$ and 1) are performed assuming the orthorhombic structure with a space group of *Pnma* (Fig. 1d–f, Tables 1 and 2). The chemically delithiated Li₀MnPO₄, however, cannot be refined because the full delithiation induces the formation of a hydrated phase, MnPO₄·H₂O, or an amorphous phase upon storage under even in an Ar atmosphere in a glove box, indicating the hydroscopic character of Li₀MnPO₄. A similar phenomenon was reported by Yamada et al. [21] in that the structural instability and loss of long-range order are caused by elastic energy accumulated inside the lattice. This is natural because olivine compounds readily absorb water molecules, which would be facilitated in the highly oxidized state. It is notable that the partial replacement of Mn by Fe significantly improves the structural stability at the fully delithiated state (Fig. 1e). Samples other than Li₀MnPO₄ are well-crystallized and are indexed by the single-phase orthorhombic *Pnma* space group (Fig. 1d and e). Other phases can be segregated as impurities such as Fe, Fe₃O₄, Fe₂O₃, Li₃Fe₂(PO₄)₃, Fe₂P [22–24]. As shown in the XRD patterns (Fig. 1d and e), the used powders do not contain impurities.

The TGA behavior of the chemically delithiated Li₀Mn_xFe_{1-x}PO₄ ($x = 0, 0.5$ and 1) with heating in an Ar atmosphere is shown in Fig. 2. Distinct weight changes for the three samples are observed up to 700 °C. Li₀FePO₄ exhibits the smallest weight loss, approximately 4.8 wt. %, over the heating range: the loss was only 1.3 wt. % up to 400 °C, after which the weight varies more significantly up to 700 °C. For Li₀Mn_{0.5}FePO₄, the resulting weight variation is more evident than that of Li₀FePO₄ up to 400 °C (~3 wt. %), and the slow

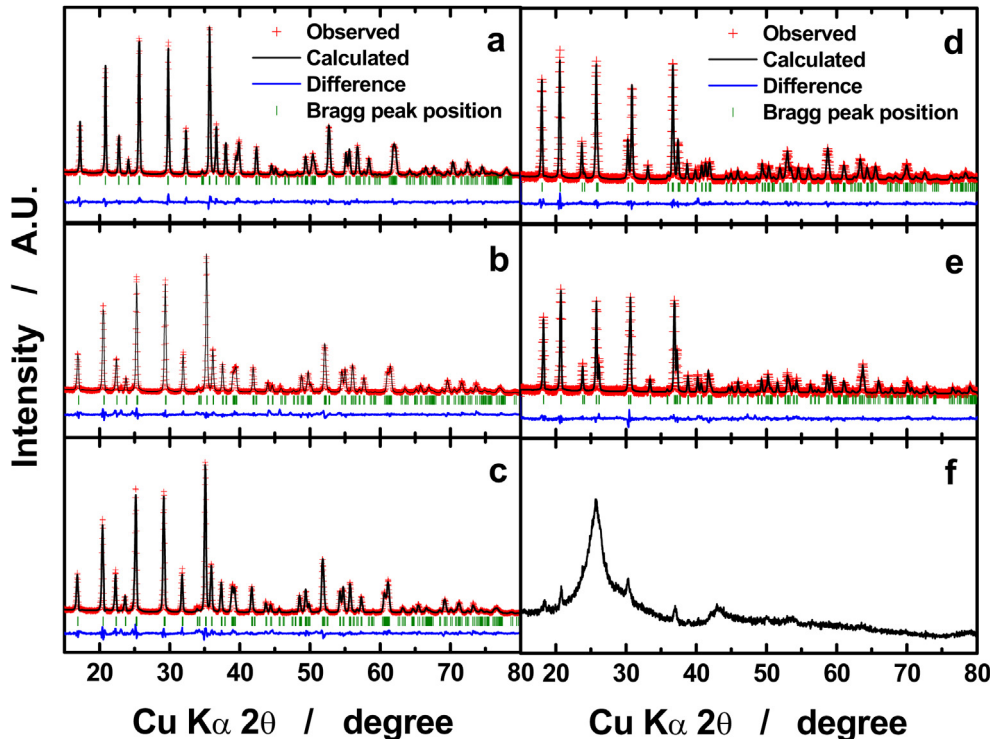


Fig. 1. Rietveld refinement data of XRD patterns of (a) as-synthesized carbon-coated (a) LiFePO₄, (b) LiFe_{0.5}Mn_{0.5}PO₄, and (c) LiMnPO₄; fully delithiated (d) Li₀FePO₄, (e) Li₀Fe_{0.5}Mn_{0.5}PO₄, and (f) XRD pattern of Li₀MnPO₄.

weight loss is nearly terminated at approximately 580 °C, with only ~2 wt. % loss. Afterward, the weight is constant to 700 °C. The total weight loss is similar for both samples during the heating. Up to 400 °C, the observed weight loss is related to oxygen release from the structure, which may result in the structural change upon heating. The oxygen release occurs more slowly and the content is less for Li₀FePO₄, implying that the structure evolves more slowly with temperature than does Li₀Mn_{0.5}Fe_{0.5}PO₄. Compared to the curves up to 100 °C, where Li₀FePO₄ exhibits a negligible weight change, the observed loss (1 wt. %) for Li₀Mn_{0.5}Fe_{0.5}PO₄ is ascribed to the evaporation of adhered water. Interestingly, this is further evidenced in Li₀MnPO₄ with approximately 1.5 wt. % loss. This experimental data confirms Yamada's suggestion that hydration of the Mn-contained olivine structure readily occurs due to its structural instability. Further change in the weight occurs aggressively up to 400 °C (~12.9 wt. %) and further continues to 700 °C (6.5 wt. %). Similar properties are observed for delithiated Li_xMnPO₄ by Chen et al. [13]. Assuming the dehydration of amorphous

MnPO₄·H₂O up to 400 °C, the observed weight loss would be associated with structural change above 400 °C.

The structural changes of the chemically delithiated Li₀Mn_xFe_{1-x}PO₄ ($x = 0, 0.5$ and 1) follow heating in an Ar atmosphere. In situ HT-XRD patterns obtained from 50 to 700 °C are shown in Figs. 3–5. A Pt sample holder is used as the internal standard for calibration of the peaks.

The Li₀FePO₄ phase maintains its structure up to 550 °C (Fig. 3a), which agrees with previous results [12,25]. The temperature is partially increased compared to that in the literature, presumably because the carbon coating layer resides on the surface of Li₀FePO₄ and impedes oxygen evolution. As shown in Fig. 2, the resulting weight loss of Li₀FePO₄ progresses slowly with temperature, which explains the structural stability of Li₀FePO₄ at an elevated temperature. When oxygen is abruptly released from the structure (600 °C in TGA curve, Fig. 2), the phase begins to decompose into two new phases, Fe^{II}₂P₂O₇ and Fe^{II}₃(PO₄)₂, up to 700 °C, and the

Table 1
Rietveld refinement results of XRD data for delithiated Li₀FePO₄.

Formula	Li ₀ FePO ₄					
Crystal system	Orthorhombic					
Space group	Pnma					
Atom	Site	x	y	z	g	B/Å ²
Fe	4c	0.274(2)	0.25	0.949(4)	1	0.9
P	4c	0.094(3)	0.25	0.396(8)	1	0.8
O1	4c	0.114(6)	0.25	0.706(16)	1	1.7
O2	4c	0.441(7)	0.25	0.164(11)	1	0.6
O3	8d	0.167(5)	0.047(8)	0.251(8)	1	0.9
Cell	$a = 9.8150(3)$ Å					
parameters	$b = 5.7892(2)$ Å					
	$c = 4.7842(2)$ Å					
R_{wp}		5.99%				
R_p		8.69%				

Table 2
Rietveld refinement results of XRD data for delithiated Li₀Fe_{0.5}Mn_{0.5}PO₄.

Formula	Li ₀ Fe _{0.5} Mn _{0.5} PO ₄					
Crystal system	Orthorhombic					
Space group	Pnma					
Atom	Site	x	y	z	g	B/Å ²
M ^a	4c	0.279(2)	0.25	0.937(5)	1	1.0
P	4c	0.096(4)	0.25	0.401(12)	1	0.7
O1	4c	0.106(9)	0.25	0.707(23)	1	1.7
O2	4c	0.442(10)	0.25	0.150(17)	1	0.6
O3	8d	0.167(7)	0.050(11)	0.243(11)	1	0.9
Cell	$a = 9.8905(3)$ Å					
parameters	$b = 5.8457(2)$ Å					
	$c = 4.8046(2)$ Å					
R_{wp}		7.37%				
R_p		9.89%				

^a It denotes transition metals (Fe, Mn).

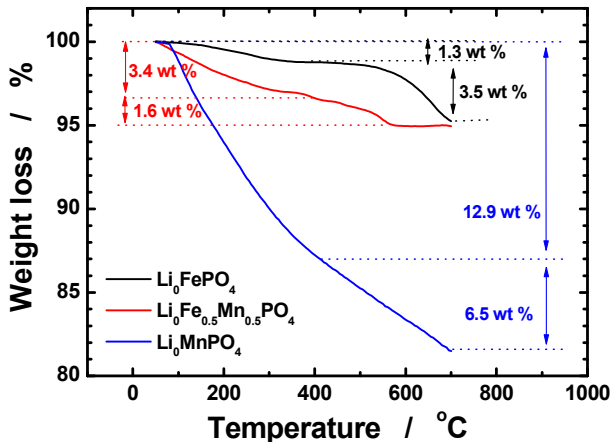


Fig. 2. Thermogravimetric curves of fully delithiated Li_0FePO_4 , $\text{Li}_0\text{Fe}_{0.5}\text{Mn}_{0.5}\text{PO}_4$, Li_0MnPO_4 . The measurements were conducted in an Ar atmosphere.

original olivine Li_0FePO_4 structure is not detected at 700 °C (Fig. 3a and b). Despite the trivalent oxidation state of Fe for Li_0FePO_4 , the oxidation state of Fe is divalent for the newly formed $\text{Fe}^{II}_2\text{P}_2\text{O}_7$ and $\text{Fe}^{II}_3(\text{PO}_4)_2$ compounds. Since the measured environment was a reduction atmosphere, the divalent Fe-containing products are

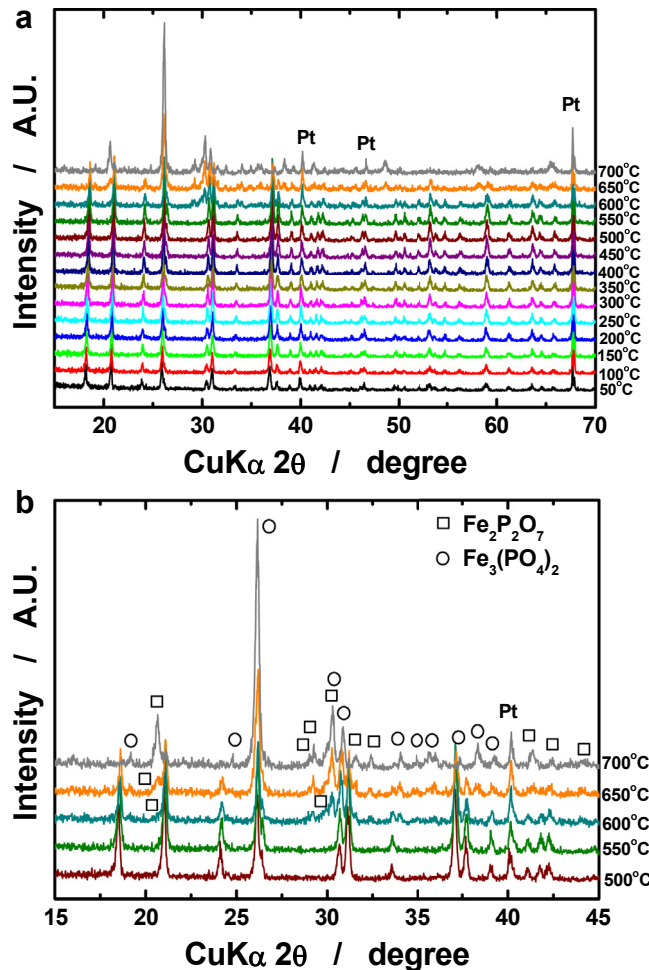


Fig. 3. (a) High temperature in-situ XRD patterns of chemically delithiated Li_0FePO_4 and (b) a highlighted portion from 15 to 45° (2 theta) over 550–700 °C.

formed. Otherwise, the products would be trivalent oxide forms because of the low sublimation temperature of phosphorus oxide in air.

The delithiated $\text{Li}_0\text{Mn}_{0.5}\text{Fe}_{0.5}\text{PO}_4$ represents different variations in structure with heating (Fig. 4). Reduced relative intensities for the XRD patterns (Fig. 4a) are obvious compared to that for Li_0FePO_4 (Fig. 3a), although no significant structural change occurred. Structural change does not occur at temperatures less than 200 °C (Fig. 4a), above which a new phase, $(\text{Mn}_{0.5}\text{Fe}_{0.5})_3(\text{PO}_4)_2$, appears. The diffraction intensity of $(\text{Mn}_{0.5}\text{Fe}_{0.5})_3(\text{PO}_4)_2$ is maximized at 300 °C, though the phase nearly disappears at 400 °C. Considering the weight loss is approximately 3 wt. % up to 400 °C including water evaporation, the oxygen loss from the $\text{Li}_0\text{Mn}_{0.5}\text{Fe}_{0.5}\text{PO}_4$ induces partial formation of the $(\text{Mn}_{0.5}\text{Fe}_{0.5})_3(\text{PO}_4)_2$ structure in the $\text{Li}_0\text{Mn}_{0.5}\text{Fe}_{0.5}\text{PO}_4$ matrix. Formations of $(\text{Mn}_{0.5}\text{Fe}_{0.5})\text{P}_4\text{O}_{11}$ and $(\text{Mn}_{0.5}\text{Fe}_{0.5})_2\text{P}_2\text{O}_7$ are initiated from 450 °C, and the $(\text{Mn}_{0.5}\text{Fe}_{0.5})_2\text{P}_2\text{O}_7$ phase becomes dominant from 600 °C, though $(\text{Mn}^{II}_{0.5}\text{Fe}^{II}_{0.5})\text{P}_4\text{O}_{11}$ is extinguished at 650 °C. Above this temperature, only $(\text{Mn}_{0.5}\text{Fe}_{0.5})_2\text{P}_2\text{O}_7$ is observed in the XRD pattern (Fig. 4b), indicating termination of the phase transformation. In comparison with the TGA data in Fig. 2, the resulting weight does not vary above 580 °C, which reflects the stability of the $(\text{Mn}_{0.5}\text{Fe}_{0.5})_2\text{P}_2\text{O}_7$ structure at high temperature.

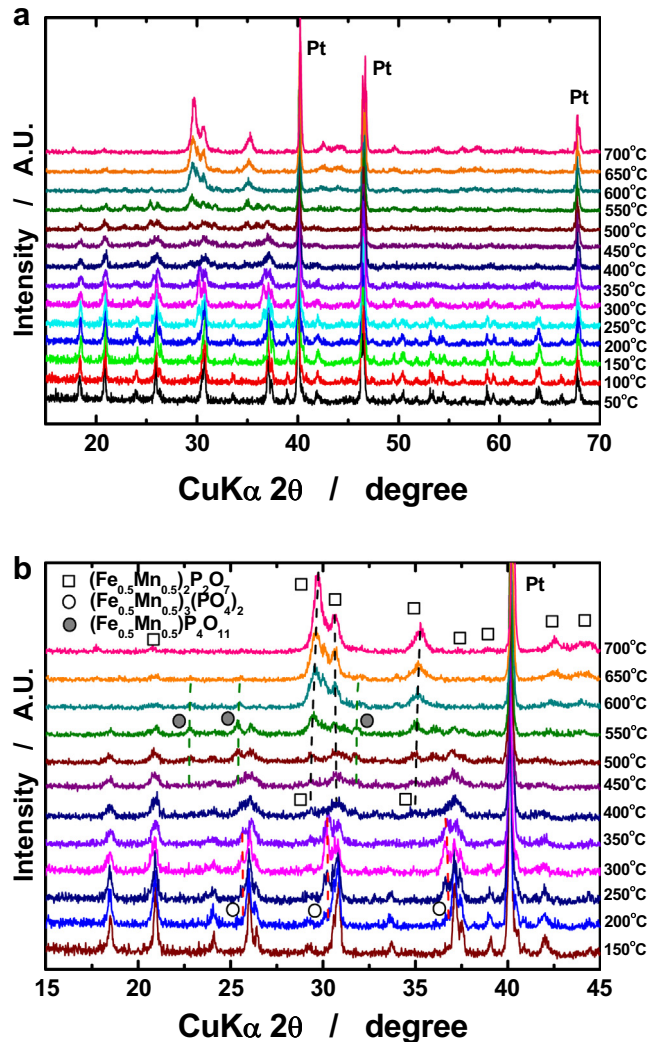


Fig. 4. (a) High temperature in-situ XRD patterns of chemically delithiated $\text{Li}_0\text{Fe}_{0.5}\text{Mn}_{0.5}\text{PO}_4$ and (b) a highlighted portion from 15 to 45° (2 theta) over 200–700 °C.

For the amorphous Li_0MnPO_4 , detection of crystalline peaks is difficult when heating to 400 °C (Fig. 5a). Interestingly, minor changes are perceived starting at 450 °C; primarily, the crystallization initiation of $\text{Mn}^{\text{II}}_3(\text{PO}_4)_2$ (26.8° and 26.5° , 2θ) and $\text{Mn}^{\text{II}}_2\text{P}_2\text{O}_7$ (29° , 2θ), shown in Fig. 5b. The large weight loss up to 400 °C in the TGA curve (Fig. 2) is primarily due to the removal of crystal water formed in the amorphous $\text{MnPO}_4 \cdot \text{H}_2\text{O}$. The crystalline phases then start to form at 450 °C. Both phases are major components with further increases in temperature, with approximately 6.5 wt. % weight loss to 700 °C. The relative diffraction intensity of the $\text{Mn}_3(\text{PO}_4)_2$ phase is slightly diminished compared to the intensity observed at 600 °C, whereas the intensity is the greatest at 700 °C for the $\text{Mn}_2\text{P}_2\text{O}_7$ phase, implying better thermal stability of the $\text{Mn}^{\text{II}}_2\text{P}_2\text{O}_7$ phase at high temperature, which is consistent with the results of $(\text{Mn}_{0.5}\text{Fe}_{0.5})_2\text{P}_2\text{O}_7$ (Fig. 4b).

Structural evolution for the $\text{Li}_0\text{Mn}_x\text{Fe}_{1-x}\text{PO}_4$ ($x = 0, 0.5$ and 1) analyzed by the in situ HT-XRD study is summarized (Fig. 6). The delithiated olivines experience different thermal behavior upon heating. The original olivine structure of Li_0FePO_4 is stable up to 550 °C and shows the smallest variation in weight (1.6 wt. %) with temperature among the delithiated samples (Fig. 2). The range is significantly narrowed to as low as 150 °C by the addition of Mn in

FePO_4 , wherein approximately 1.4 wt. % weight loss is derived from oxygen release from the structure. Above those temperatures, common for both delithiated samples, even slight oxygen loss induces the partial formation of the $\text{M}_3(\text{PO}_4)_2$ ($\text{M} = \text{Fe}$ and $\text{Mn}_{0.5}\text{Fe}_{0.5}$) phase, 600 °C (0.6 wt. % from 550 °C, total 2.2 wt. %) for Li_0FePO_4 and 200 °C (0.6 wt. % from 150 °C, total 2 wt. %) for $\text{Li}_0\text{Mn}_{0.5}\text{Fe}_{0.5}\text{PO}_4$.

For Li_0FePO_4 , the oxygen release occurs drastically above 550 °C so that the $\text{Fe}_2\text{P}_2\text{O}_7$ phase is observed with $\text{Fe}_3(\text{PO}_4)_2$ starting at 600 °C. At 700 °C, the original olivine structure is not observed, and only $\text{Fe}_3(\text{PO}_4)_2$ and $\text{Fe}_2\text{P}_2\text{O}_7$ phases appear. In contrast, the oxygen loss progresses slowly from 150 to 550 °C for $\text{Li}_0\text{Mn}_{0.5}\text{Fe}_{0.5}\text{PO}_4$. As a result, distinct phase transformation from $\text{Li}_0\text{Mn}_{0.5}\text{Fe}_{0.5}\text{PO}_4$ toward $(\text{Mn}_{0.5}\text{Fe}_{0.5})_2\text{P}_2\text{O}_7$ via $(\text{Mn}_{0.5}\text{Fe}_{0.5})_3(\text{PO}_4)_2$ and $(\text{Mn}_{0.5}\text{Fe}_{0.5})\text{P}_4\text{O}_{11}$ intermediate phases in the sequence is observed with oxygen loss from the structure. The above-mentioned structural evolution, however, could not be defined with temperature because the weight loss is primarily associated with dehydration of amorphous $\text{MnPO}_4 \cdot \text{H}_2\text{O}$ up to 400 °C for Li_0MnPO_4 . Similar to Li_0FePO_4 , oxygen evaporates fast from Li_0MnPO_4 , so that both $\text{Mn}_3(\text{PO}_4)_2$ and $\text{Mn}_2\text{P}_2\text{O}_7$ phases present at 700 °C, though $\text{Mn}_2\text{P}_2\text{O}_7$ is more stable at a high temperature as is confirmed from the maximized intensity in XRD patterns (Fig. 5). This series of phase transformations is facilitated by the addition of Mn in the Li_0FePO_4 lattice, in which the added Mn disintegrates the long-range order in the crystal structure. As a result, the $\text{Li}_0\text{Mn}_x\text{Fe}_{1-x}\text{PO}_4$ ($x = 0, 0.5$ and 1) structure is finally stabilized to $\text{M}_2\text{P}_2\text{O}_7$ ($\text{M} = \text{Fe}$, $\text{Mn}_{0.5}\text{Fe}_{0.5}$, and Mn) resulting from the oxygen loss from the lithium-free olivine structure at high temperature.

DSC data are compared for the chemically delithiated $\text{Li}_0\text{Mn}_x\text{Fe}_{1-x}\text{PO}_4$ ($x = 0$ and 0.5) in the presence of 1 M LiPF_6 in ethylene carbonate/diethyl carbonate electrolyte (3 mg) in Fig. 7, because exothermic reactions were hardly observed for the chemically delithiated olivines without electrolyte. Li_0MnPO_4 is excluded from the measurement due to the high amount of water absorption resulting in amorphous $\text{MnPO}_4 \cdot \text{H}_2\text{O}$. Both delithiated olivines are thermally stable over a wide temperature range of 150–350 °C with low exothermic heats of 92 and 148 J g⁻¹ for Li_0FePO_4 and $\text{Li}_0\text{Mn}_{0.5}\text{Fe}_{0.5}\text{PO}_4$, respectively. The thermal behavior of these delithiated olivines can be interpreted based on the in situ HT-XRD and TGA data. For Li_0FePO_4 , the lost oxygen is less than 1.3 wt. % up to 350 °C, and the original olivine structure is maintained at this temperature. The associated exothermic reaction, therefore, occurs because of the simple oxygen release from the structure. In contrast, a relatively large amount of oxygen (3 wt. %) is lost from the $\text{Li}_0\text{Mn}_{0.5}\text{Fe}_{0.5}\text{PO}_4$ structure up to 350 °C, accompanied by the

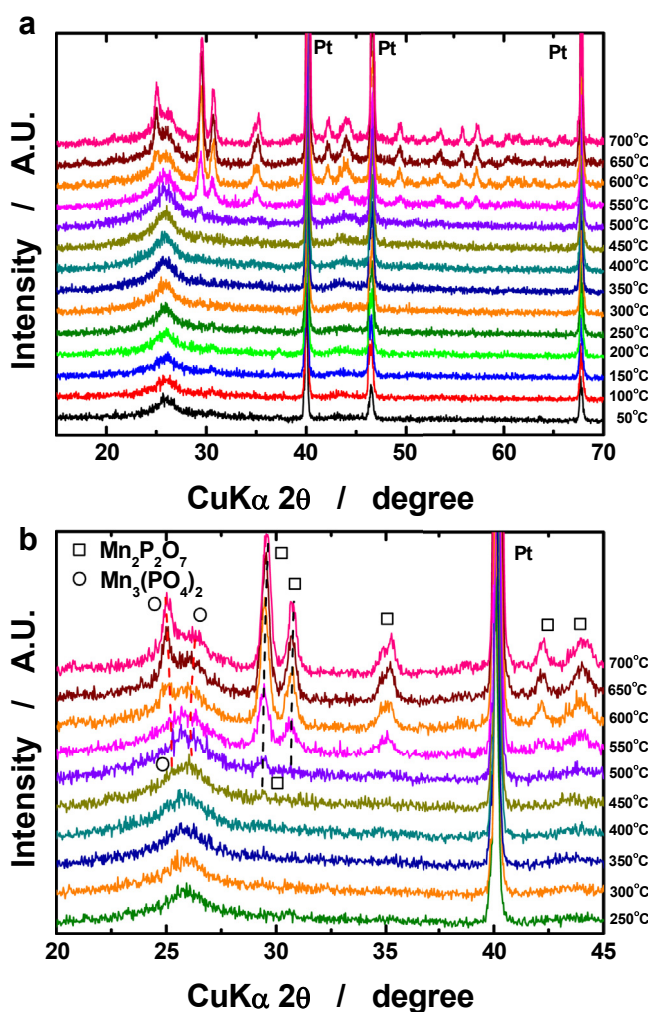


Fig. 5. (a) High temperature in-situ XRD patterns of chemically delithiated Li_0MnPO_4 and (b) a highlighted portion from 20 to 45° (2θ) over 250–700 °C.

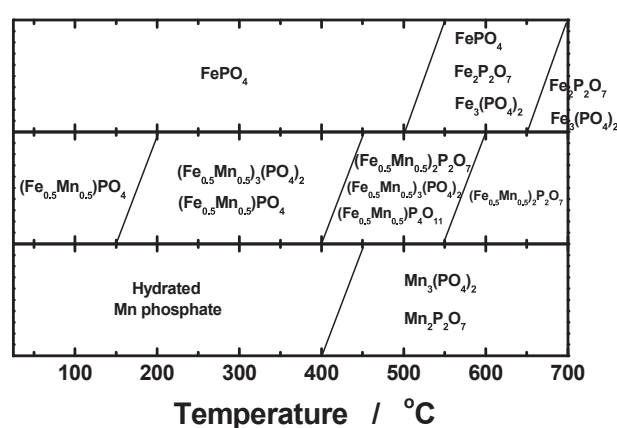


Fig. 6. Summary of the phase evolution with temperature based on the results of Figs. 3–5.

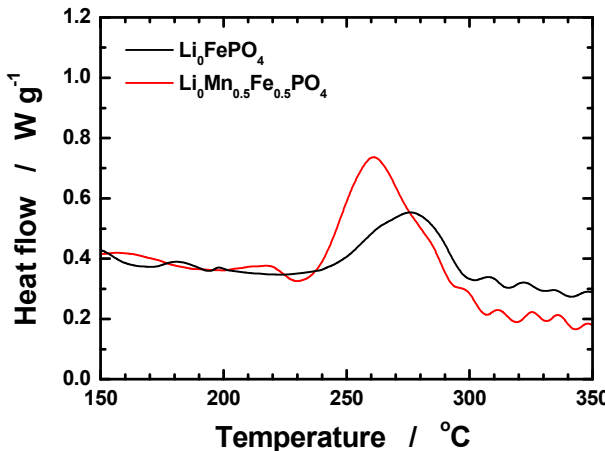


Fig. 7. DSC curves of fully delithiated Li₀FePO₄ and Li₀Fe_{0.5}Mn_{0.5}PO₄. For the measurement, 3 mg of electrolyte was added.

phase transformation to (Mn_{0.5}Fe_{0.5})₃(PO₄)₂. For these reasons, the better thermal stability of Li₀FePO₄ is attributed to less oxygen loss that delays the phase transformation, resulting in less exothermic heat in the temperature range. It is notable that the evolved oxygen contents are similar to those of delithiated Li_{0.35}[Ni_{1/3}Co_{1/3}Mn_{1/3}]O₂ layer compounds in the same temperature range [26], where the layer structure transforms to spinel with a significant exothermic heat generation at least 10 times greater than those of the olivines. Although the oxygen evolution results in phase transformation to (Mn_{0.5}Fe_{0.5})₃(PO₄)₂ with little exothermic heat, the presence of oxygen at a similar level as the layer compound may not be favored, even in hermetically-sealed cells. This thermal concern of composition should be considered because the thermally stable olivine-type LiMn_xFe_{1-x}PO₄ ($x = 0\text{--}1$) is one of the most appropriate candidates for the cathode materials of large-format batteries for energy storage systems.

4. Conclusions

The thermal behavior of chemically delithiated carbon-coated Li₀Mn_xFe_{1-x}PO₄ ($x = 0$ and 0.5) is demonstrated using TGA, in situ XRD, and DSC studies. The delithiated olivines are thermally stable in exothermic heat due to the presence of covalent bonds in the structure, though phase transformation accompanies the Li₀Mn_{0.5}Fe_{0.5}PO₄ to the (Mn_{0.5}Fe_{0.5})₃(PO₄)₂ phase. This tendency is not observed for Mn-free Li₀FePO₄ in the temperature range of 150–350 °C because of less oxygen released from the structure. A detailed thermal investigation for Li₀MnPO₄ is not easy due to readily adsorbed water during sample handling and measurement. The mechanism of the thermal stability of the delithiated

Li₀Mn_xFe_{1-x}PO₄ ($x = 0$ and 0.5) is comprehensively understood through this study.

Acknowledgments

This research was supported by the National Research Foundation of Korea funded by the Korean government (MEST) (NRF-2009-C1AAA001-0093307), the Basic Science Research Program through the National Research Foundation of Korea (NRF) funded by the Ministry of Education, Science and Technology (2011-0024683), and the National Research Foundation of Korea (NRF) grant funded by the Korea government (MSIP) for the Center for Next Generation Dye-sensitized Solar Cells (No. 2008-0061903). This work was also partially supported by the IT R&D Program of MKE/KEIT (10041856).

References

- [1] A.K. Padhi, K.S. Nanjundaswamy, J.B. Goodenough, *J. Electrochem. Soc.* 144 (1997) 1188.
- [2] S.-Y. Chung, J.T. Bloking, Y.-M. Chiang, *Nat. Mater.* 1 (2002) 123.
- [3] H. Huang, S.C. Yin, L.F. Nazar, *Electrochem. Solid-State Lett.* 4 (2001) A170.
- [4] Z. Chen, J.R. Dahn, *J. Electrochem. Soc.* 149 (2002) A1884.
- [5] A. Yamada, Y. Kudo, K.Y. Liu, *J. Electrochem. Soc.* 148 (2001) A747.
- [6] T. Shiratsuchi, S. Okada, T. Doi, J. Yamaki, *Electrochim. Acta* 54 (2009) 3145.
- [7] C. Delacourt, L. Laffont, R. Bouchet, C. Wurm, J.-B. Leriche, M. Morcrette, J.-M. Tarascon, C. Masquelier, *J. Electrochem. Soc.* 152 (2005) A913.
- [8] M. Yonemura, A. Yamada, Y. Takei, N. Sonoyama, R. Kanno, *J. Electrochem. Soc.* 151 (2004) A1352.
- [9] S.K. Martha, B. Markovsky, J. Grinblat, Y. Gofer, O. Haik, E. Zinigrad, D. Aurbach, T. Drezen, D. Wang, G. Deghenghi, I. Exnar, *J. Electrochem. Soc.* 156 (2009) A541.
- [10] S.K. Martha, J. Grinbalt, O. Haik, E. Zinigrad, T. Drazen, J.H. Miners, I. Exnar, A. Kay, B. Markovsky, D. Aurbach, *Angew. Chem. Int. Ed.* 48 (2009) 8559.
- [11] Y. Wang, Y. Yang, Y. Yang, H. Shao, *Mater. Res. Bull.* 44 (2009) 2139.
- [12] G. Rousse, J. Rodriguez-Garvajal, S. Patoux, C. Masquelier, *Chem. Mater.* 15 (2003) 4082.
- [13] G. Chen, T.J. Richardson, *J. Electrochem. Soc.* 156 (2009) A756.
- [14] S.-W. Kim, J. Kim, H. Gwon, K. Kang, *J. Electrochem. Soc.* 156 (2009) A635.
- [15] S.-M. Oh, S.-T. Myung, J.B. Park, B. Scrosati, K. Amine, Y.-K. Sun, *Angew. Chem. Int. Ed.* 51 (2012) 1853.
- [16] S.W. Oh, S.-T. Myung, S.-M. Oh, K.H. Oh, K. Amine, B. Scrosati, Y.-K. Sun, *Adv. Mater.* 22 (2010) 4842.
- [17] S.-M. Oh, S.-T. Myung, Y.-S. Choi, K.-H. Oh, Y.-K. Sun, *J. Mater. Chem.* 21 (2011) 19368.
- [18] S.-M. Oh, H.-G. Jung, C.S. Yoon, S.-T. Myung, Z. Chen, K. Amine, Y.-K. Sun, *J. Power Sources* 196 (2011) 6924.
- [19] T. Roisnel, J. Rodriguez-Carval, *Fullprof Manual*, Institut Laue-Langevin, Grenoble, 2002.
- [20] R.D. Shannon, *Acta Crystallogr. Sect. A Cryst. Phys. Diffraction Theory Gen. Crystallogr.* 32 (1976) 756.
- [21] A. Yamada, Y. Takei, H. Koizumi, N. Sonoyama, R. Kanno, *Chem. Mater.* 18 (2006) 804.
- [22] A. Yamada, S.-C. Chung, K. Hinokuma, *J. Electrochem. Soc.* 148 (2001) A224.
- [23] P.S. Herle, B. Ellis, N. Coombs, L. Nazar, *Nat. Mater.* 3 (2004) 147.
- [24] K. Dokko, K. Shiraishi, K. Kanamura, *J. Electrochem. Soc.* 152 (2005) A2199.
- [25] J. Kim, K.-Y. Park, I. Park, J.-K. Yoo, J. Hong, K. Kang, *J. Mater. Chem.* 22 (2012) 11964.
- [26] S.-T. Myung, K.-S. Lee, C.S. Yoon, Y.-K. Sun, K. Amine, H. Yashiro, *J. Phys. Chem. C* 114 (2010) 4170.